phys. stat. sol. (a) **201**, No. 7, 1518–1527 (2004) / **DOI** 10.1002/pssa.200306799

Influence of alloying elements on the structure and corrosion resistance of galvanized coatings

G. Vourlias[1], **N. Pistofidis**[1], **G. Stergioudis**[*, 1], **E. Pavlidou**[1], and **D. Tsipas**[2]

[1] Physics Department, Aristotle University of Thessaloniki, 54124, Thessaloniki, Greece
[2] Mechanical Engineering Department, Aristotle University of Thessaloniki, 54124, Thessaloniki, Greece

Received 12 November 2003, accepted 26 February 2004
Published online 11 May 2004

PACS 61.10.Nz, 68.35.Fx, 68.37.Hk, 81.15.–z, 81.65.Kn

Carbon steel samples were galvanized by the hot-dip method in zinc baths containing 0.5 or 1 wt% aluminum, copper, tin, nickel, and/or lead. Bath temperature ranged from 450 to 480 °C. The samples were examined using optical microscopy, scanning electron microscopy (SEM) and X-ray diffraction (XRD). The influence of the alloying elements on the formation of the different phases and on the diffusion process is discussed. In order to study the kinetics and the mechanism of corrosion of these materials, corrosion experiments were carried out in a simulated environment of accelerated atmospheric corrosion conditions, for which a special chamber (Salt Spray Chamber – Alternative Climate Test Chamber) of type SC-450 was used. The corroded samples were examined using optical microscopy, SEM and XRD. Chloride and oxide phases, which penetrated the materials to different depths from the surface, were revealed. Finally, useful conclusions were drawn which help to control the factors of the corrosion behavior of the examined materials in a marine atmosphere.

1 Introduction

Hot-dip galvanizing is one of the most common processes for the corrosion protection of steel and iron substrates. The hot-dip galvanizing process consists of three basic steps [1, 2]: the surface preparation of the ferrous substrate, the hot-dipping (galvanizing), and the post-treatment. Surface preparation includes three steps: degreasing of the substrate through alkaline or acid cleaning, removal of the scale and the rust through pickling with an inorganic acid, and fluxing with an aqueous solution of $ZnCl_2 \cdot 2NH_4Cl$ or $ZnCl_2 \cdot 3NH_4Cl$. After surface preparation the ferrous material is galvanized, e.g. immersed in a bath of almost pure molten zinc at a temperature of about 449–470 °C. Through this process, the material is covered with a layer of zinc, which protects the steel by acting as a barrier and a sacrificial anode simultaneously.

During galvanizing the molten zinc "reacts" with the iron and as a result a series of different zinc/iron phases is formed. These phases are characterized by the Greek letters η (eta), ζ (zeta), δ (delta), Γ (gamma) and Γ_1 and have different compositions (richer in iron closer to the steel substrate) [1, 2].

Nevertheless, the presence of alloying elements in the galvanizing bath has been shown to affect strongly the microstructure of the zinc coating [2–9]. Among the most widely encountered elements are aluminum, lead, tin, copper, and nickel. These elements are present either as impurities originating from the raw materials used or as alloying additions dissolved in the zinc bath since industrial experience has proven that they improve the macroscopic image of the coating (e.g. they increase the brightness of the coating). The effect of Al in low concentration (up to 0.3 wt%) has been reviewed elsewhere ([2] and references therein), [3] and it has been proven that Al causes significant changes in the microstructure of

[*] Corresponding author: e-mail: gst@auth.gr, Phone: ++30 2310 998085, Fax: ++30 2310 998003

the coating, by inhibiting the formation of the brittle Fe–Zn phases. As a result the final product is composed only by the η phase, which is separated from the substrate by a layer of an intermetallic compound with the chemical formula $Fe_2Al_5Zn_x$. Furthermore, the effect of Sn and Cu up to 3.0 wt% was studied [4] and it was found that tin does not affect the morphology of the coating, while copper causes structural changes. Nickel up to 0.1% has also been found to influence the morphology of the galvanized coating, especially when the concentration of silicon and phosphorus in the steel is low [5, 6].

In the present investigation coatings resulting from galvanizing baths containing 0.5 or 1.0 wt% of Al, Pb, Sn, Cu, and/or Ni additions were examined. The structure of the coatings has been studied. Afterwards, the specimens have been exposed in a simulated environment under accelerated corrosion conditions in order to examine the possible influence of the alloying elements on the corrosion behavior of the coating. Such a study, apart from its theoretical importance, offers useful information for applications, since the effect of the additions on the structure and the corrosion resistance of the galvanized coatings is hardly considered.

2 Experimental

Hot-rolled sheets of steel containing 0.11% C, 0.55% Mn, 0.012% Si, 0.016% P have been galvanized in a laboratory electric furnace (Thermolyne 1400) inside a graphite crucible. The dipping time varied from several seconds to about 1 min. The specimens, 60 mm long, 7 mm wide and 3 mm thick, were initially sandblasted. Afterwards, they were degreased in a solution of a non-ionic tenside containing H_3PO_4, pickled in an aqueous solution containing 16% HCl, fluxed in an aqueous solution containing 50% $ZnCl_2 \cdot 2NH_4Cl$ and dried at 110 °C for 10 min, before their dipping in the galvanizing bath at a temperature of 450–460 °C. The baths were prepared by using industrial-grade zinc (99.9861% Zn, 0.01% Pb, 0.001% Cd, 0.0012% Fe, 0.0007% Cu and 0.001% Sn). The other metals were of laboratory grade.

The corrosion of the specimens under simulated conditions took place in a Salt Spray Chamber type SC-450 [10]. The corrosive medium was a 5% solution of NaCl in deionized water in order to simulate a marine atmosphere. The specimens remained in the chamber for 16 days. The conditions in the chamber were automatically altered for the first six days. The temperature varied from 35 to 40 °C while the relative humidity remained stable at 100%. For the rest of the days (7 to 16) the temperature remained stable at 40 °C and the relative humidity at 100%.

For the examination of the microstructure, cross-sections from each galvanized specimen have been cut before and after the corrosion test, mounted in bakelite and polished down to 5 μm alumina emulsion. The specimens have been etched in 2% Nital and initially observations were made using an Olympus BX60 optical microscope connected with a digital camera CCD JVC TK-C1381.

The nature of the phases has been determined by using X-ray diffraction (XRD) and scanning electron microscopy (SEM) associated with an EDAX analyzer. The XRD was accomplished using a two-cycles Seifert 3003 TT diffractometer (Fe Kα radiation, λ = 1.9363 Å). For the SEM study the specimens were examined with a 20 kV JEOL 840A SEM equipped with an Oxford ISIS 300 EDAX analyzer and the necessary software in order to perform point microanalysis, linear microanalysis or chemical mapping of the surface under examination.

3 Results and discussion

3.1 Characterization of the coatings before the corrosion process

Figure 1 shows representative optical micrographs of the coatings. Apart from the coating formed in the bath containing Al (Fig. 1a), the morphologies of the other coatings are very similar. In all cases, the coatings consist of three layers, which are clearly distinguishable.

The results of the point microanalysis for the coatings are presented in Table 1. The data of this table average 30 measurements taken from points almost equally spaced along the circumference of every phase. By combining the data of this table with the morphology of the layers, useful conclusions about their structure can be drawn. It was deduced that the coatings resulting from baths with 0.5% Pb, 0.5%

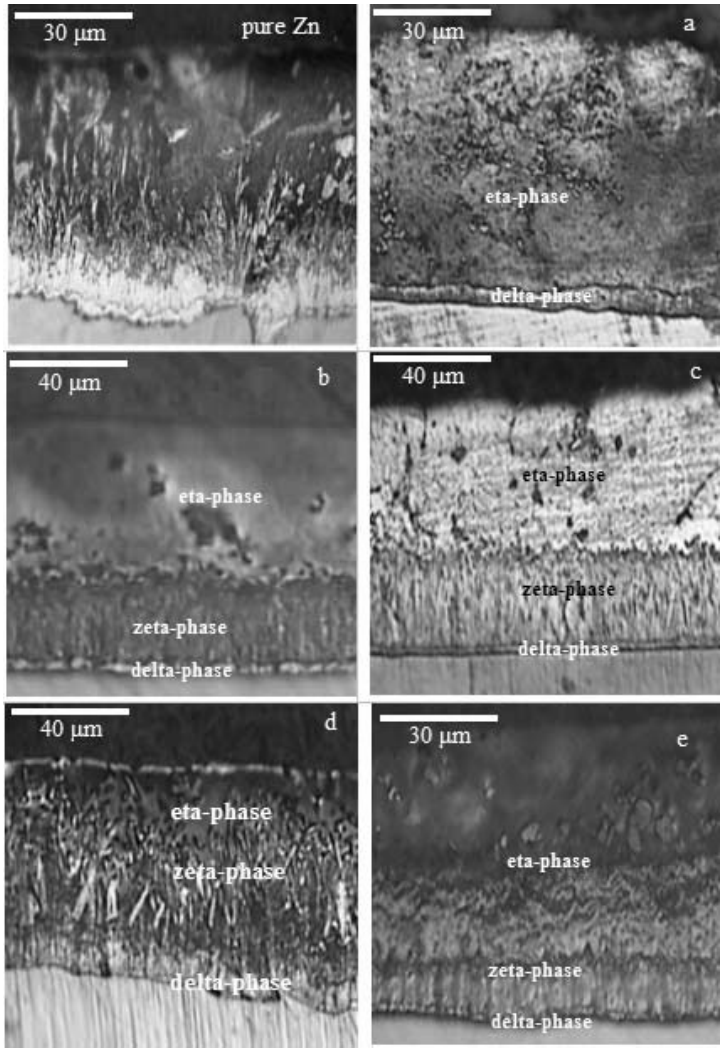

Fig. 1 Optical micrographs of the coatings formed in pure Zn (top left) and in galvanizing baths containing a) 0.5% Al, b) 0.5% Pb, c) 0.5% Sn, d) 0.5% Cu, and e) 0.5% Ni.

Sn, and 0.5% Ni, respectively, consist of the δ phase, the outer η phase and the ζ phase, which is laid between the δ and η phases having a variable thickness and structure. In some cases and for long-time immersion [2], two additional phases, the Γ and Γ_1, close to the steel surface were also observed. SEM analysis (Table 1) showed that within experimental errors the observed layers mainly belong to the δ, ζ and η phases. SEM analysis also provides additional information concerning the diffusion process of the alloying elements into the coatings and its influence on the evolution and characteristics of the formed phases. It was observed that the concentration of the elements plays a decisive role in the growth of the layers, favoring or suppressing them. This is the case mainly for Al and Ni.

Al atoms reach the surface of the steel substrate by a diffusion process, giving rise to the formation of Fe–Al or Fe–Al–Zn layers ([2] and references therein). These layers act as a barrier between substrate and zinc, inhibiting the formation of brittle Fe–Zn intermetallic phases. Finally the outer η phase, which is grown in the ⟨0001⟩ direction and consists of almost pure zinc, is favored, while the δ and ζ phases are almost suppressed. Surprisingly in the η phase several inclusions of Fe compounds were detected

Table 1 Results of the microanalysis of the coatings formed in Zn–0.5 wt% different metal baths.

	depth* (μm)	Zn (wt%)	Fe (wt%)	Al (wt%)	Pb (wt%)	Sn (wt%)	Cu (wt%)	Ni (wt%)
Zn–0.5% Al	20	99.59	0.26	0.15				
	35	98.92	0.70	0.38				
	75	89.57	8.59	1.91				
	10	98.76	0.94		0.30			
Zn–0.5% Pb	60	93.62	6.10		0.28			
	90	92.41	6.98		0.60			
Zn–0.5% Sn	20	99.22	0.36			0.42		
	85	92.14	4.92			2.93		
	120	89.93	7.39			2.68		
Zn–0.5% Cu	10	90.65	0.58				8.77	
	90	92.08	5.70				2.22	
	115	90.30	6.59				3.10	
Zn–0.5% Ni	60	99.63	0.10					0.27
	90	93.14	6.04					0.82
	110	92.03	7.93					0.04

* Calculated from the surface of the coatings.

(Table 2). XRD patterns (Fig. 2a) confirmed the (0001) basal phase texturing. Additionally some peaks corresponding to the inclusions appeared.

Ni on the other hand appears to accumulate at an intermediate distance from the substrate/surface of the coating where the ζ phase is formed. It is most probable that the nickel atoms act as nucleation sites [5] resulting in a layer composed of numerous small crystallites extended to an area ranging between the δ and η phases, while the outer η phase in this case shows a rather preferred crystallization (Fig. 2e).

Pb atoms were also found to be not uniformly distributed in the coatings, as a higher concentration was observed near the substrate/coating interface. Pb additions determine the structure of the η phase. Coatings with Pb additions show a strong texturing due to a gradual inclination of the basal (0001) plane of the η phase [7, 8]. This inclination probably results from a fast growth of the grains in thermodynamically favored directions laid within the (0001) basal plane of the zinc lattice. XRD measurements clearly revealed that the $(2\bar{1}\bar{1}1)$ planes (101 Miller indices), which consist of very large grains, are almost perfectly parallel to the sheet surface (Fig. 2b). Moreover Pb additions delay the fast thickening of the solid layer, as Pb lowers the surface tension and promotes a planar growth [2, 7, 8]. Thus Pb seems to improve the quality of the coatings (larger grains) and to produce a thinner layer.

Tin additions seem to have no obvious effect on the coating (Figs. 1c and 2c) while Cu atoms substitute for Zn ones in the outer phase, leading to a slight change of the interplanar distances (Fig. 2d).

In the case of 1.0 wt% additions only the alloying with Al atoms showed different morphology and structure compared to those containing 0.5 wt% additions (Figs. 3a and b). Microanalysis revealed that it is most probable that an intermetallic phase with the chemical formula $Fe_2Al_5Zn_x$ was formed near the

Table 2 Results of the microanalysis of an inclusion formed in the Zn–0.5% Al coating 38 μm from the coating surface.

element	concentration (wt%)
Zn	18.10
Fe	32.85
Al	49.04

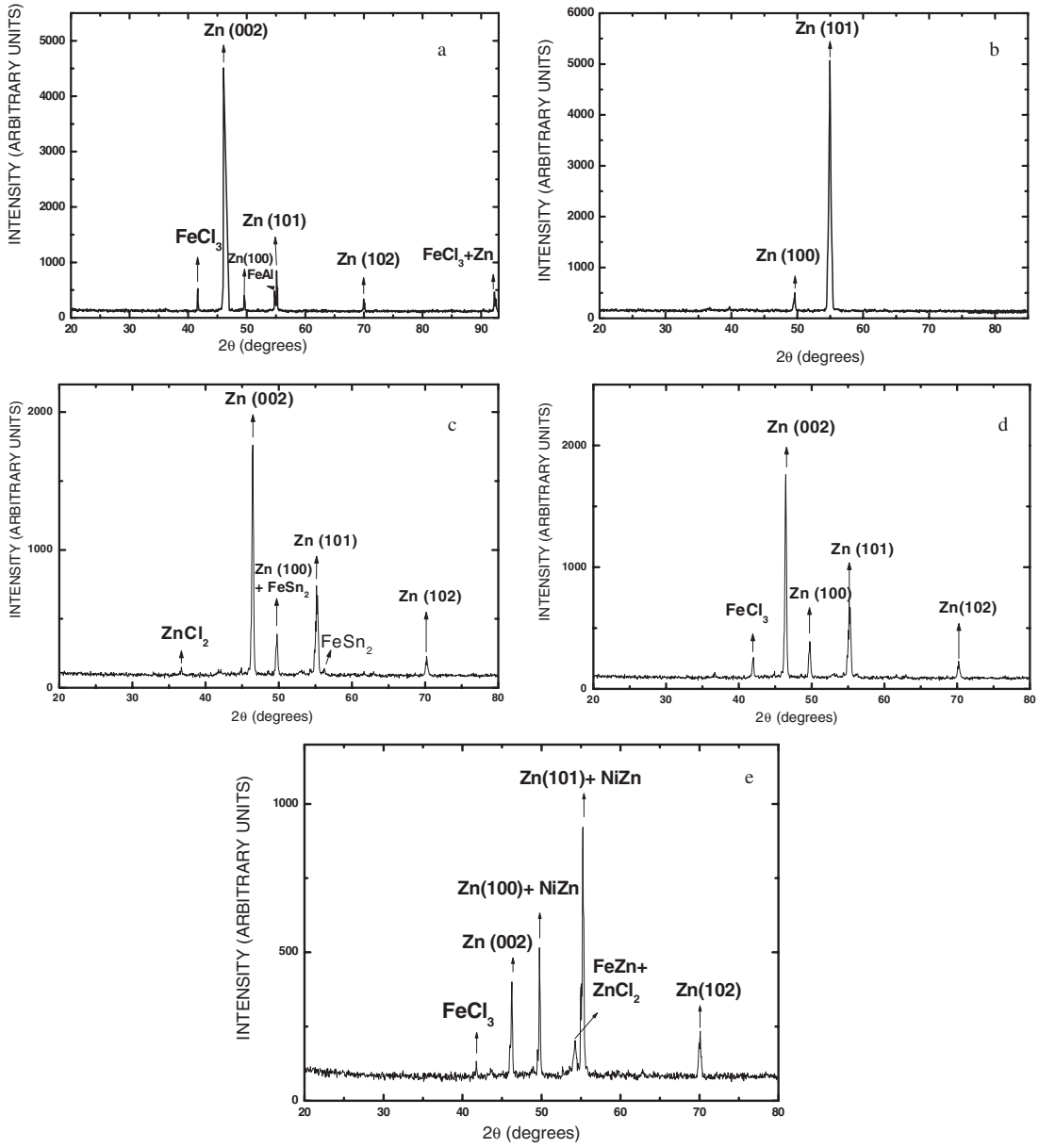

Fig. 2 X-ray diffraction patterns of the coatings formed in galvanizing baths containing a) 0.5 wt% Al, b) 0.5 wt% Pb, c) 0.5 wt% Sn, d) 0.5 wt% Cu, and e) 0.5 wt% Ni.

substrate/interface in the case of 1.0 wt% [11, 12]. This compound it is known to be very unstable. Nevertheless, in our case its lifetime increased probably because of the greater Al content.

3.2 Characterization of the materials after corrosion

It is well known that zinc, during its exposure in the atmosphere, is covered with a film of zinc compounds such as ZnO and $ZnCO_3$ [2, 13–16]. These compounds are highly insoluble in water and therefore isolate the "sensitive" substrate from the aggressive environment. This film constitutes a very important factor concerning the anticorrosive action of zinc coatings. However, it is affected by certain

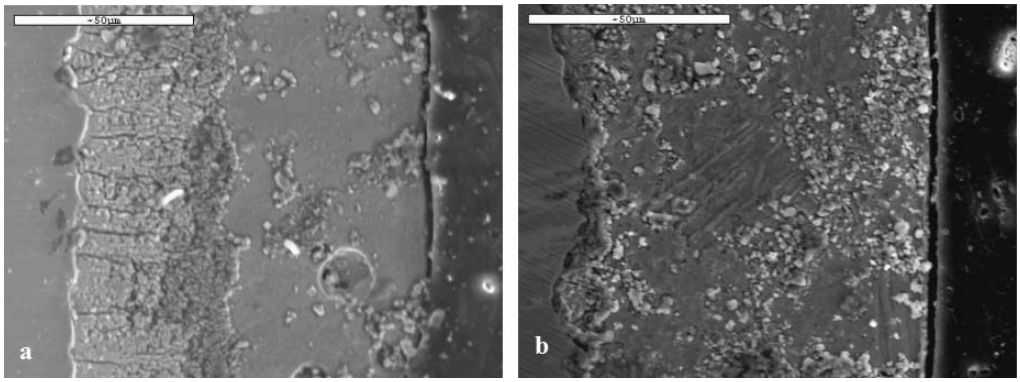

Fig. 3 SEM micrographs of the coatings formed in galvanizing baths containing a) 0.5 wt% Al and b) 1.0 wt% Al.

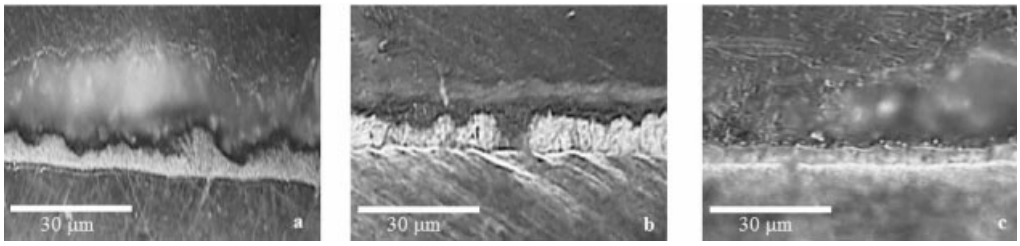

Fig. 4 Optical micrographs of the corroded coatings formed in galvanizing baths containing a) 0.5 wt% Al, b) 0.5 wt% Pb, and c) 0.5 wt% Ni.

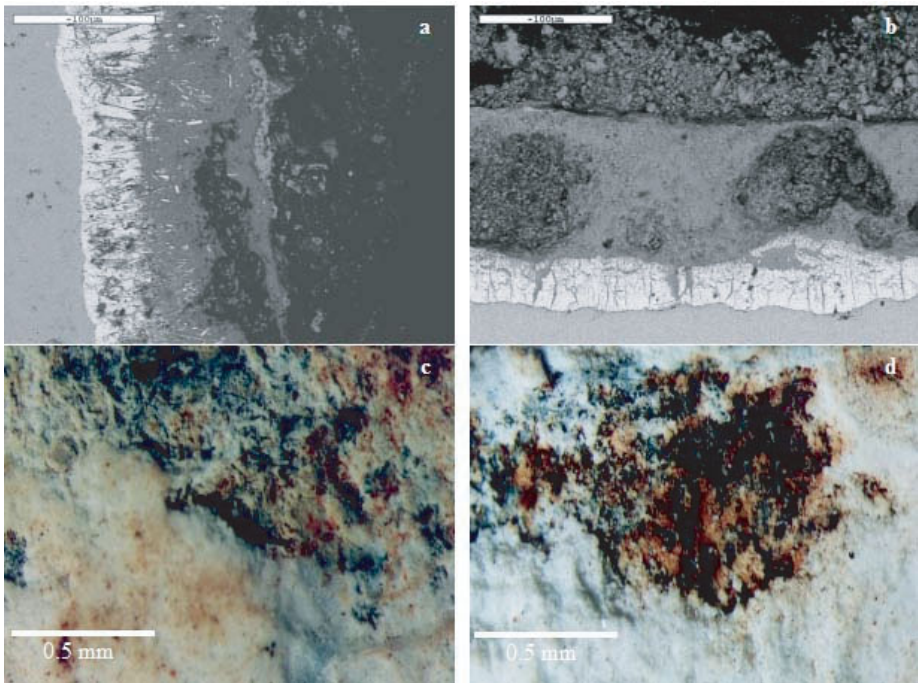

Fig. 5 (online color at: www.interscience.wiley.com) a), b) SEM micrographs of the corroded coatings formed in galvanizing baths containing a) 0.5 wt% Al and b) 0.5 wt% Sn; and c), d) macroscopic photographs (showing details of the surface) of the corroded coating that was formed in a Zn–Ni bath.

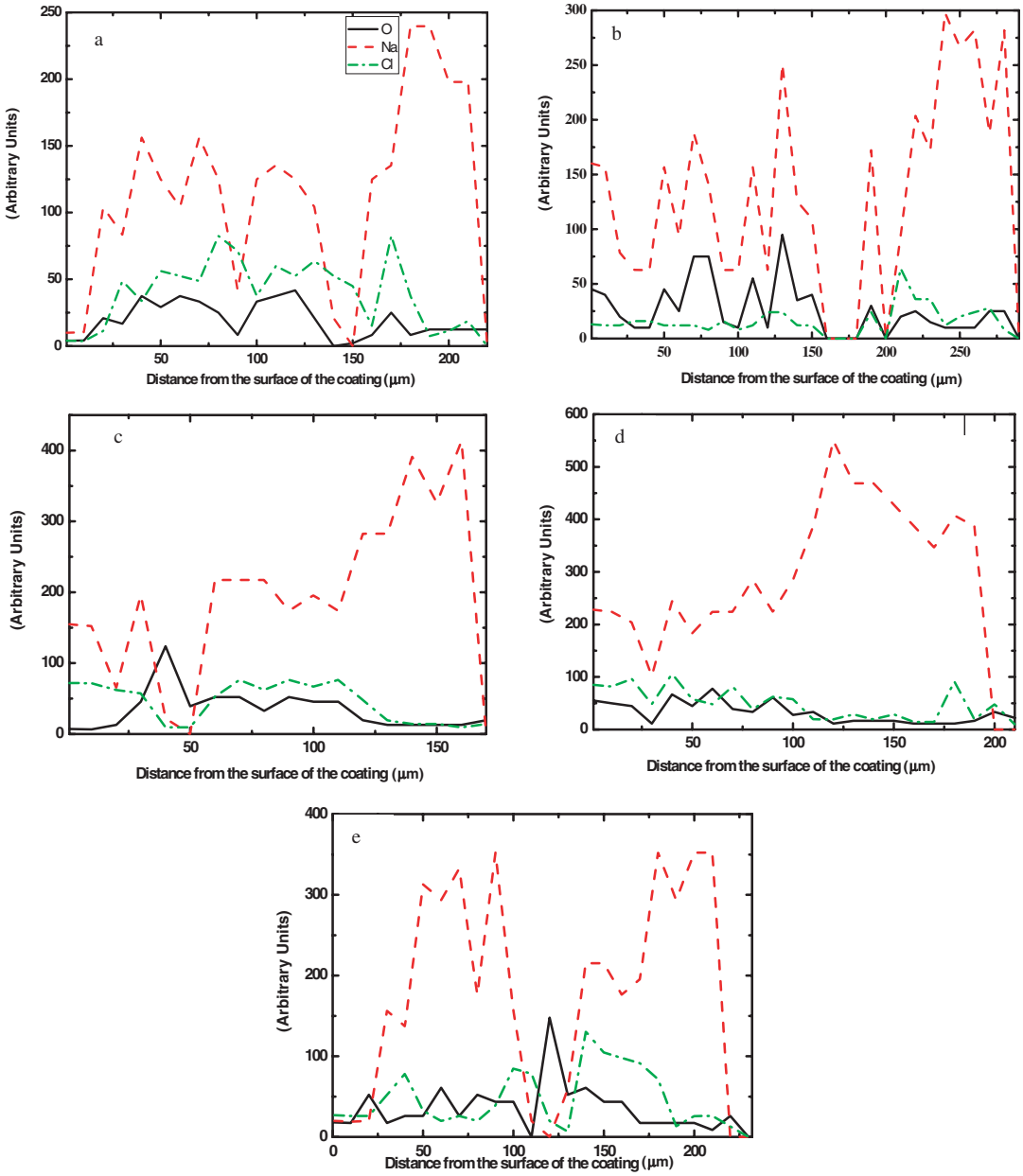

Fig. 6 (online color at: www.interscience.wiley.com) Linear microanalysis of corroded specimens: a) Zn–0.5 wt% Al, b) Zn–0.5 wt% Pb, c) Zn–0.5 wt% Sn, d) Zn–0.5 wt% Cu, and e) Zn–0.5 wt% Ni.

ionic species [13–16]. Among them the most aggressive are the Cl^- and SO_4^{2-} ions. These ions react with the protective film and as a result they form water-soluble compounds. Hence, the protective action of the film is destroyed and corrosion proceeds very quickly. This phenomenon was observed in the case of specimens that were subjected to an accelerated corrosion process.

A typical symptom of failure of a galvanized coating is the appearance of red-brown spots. The phenomenon manifests after an exposure of several years under atmospheric conditions [2]. In the case of accelerated corrosion in a salt spray chamber, the same behavior appeared after 16 days of exposure.

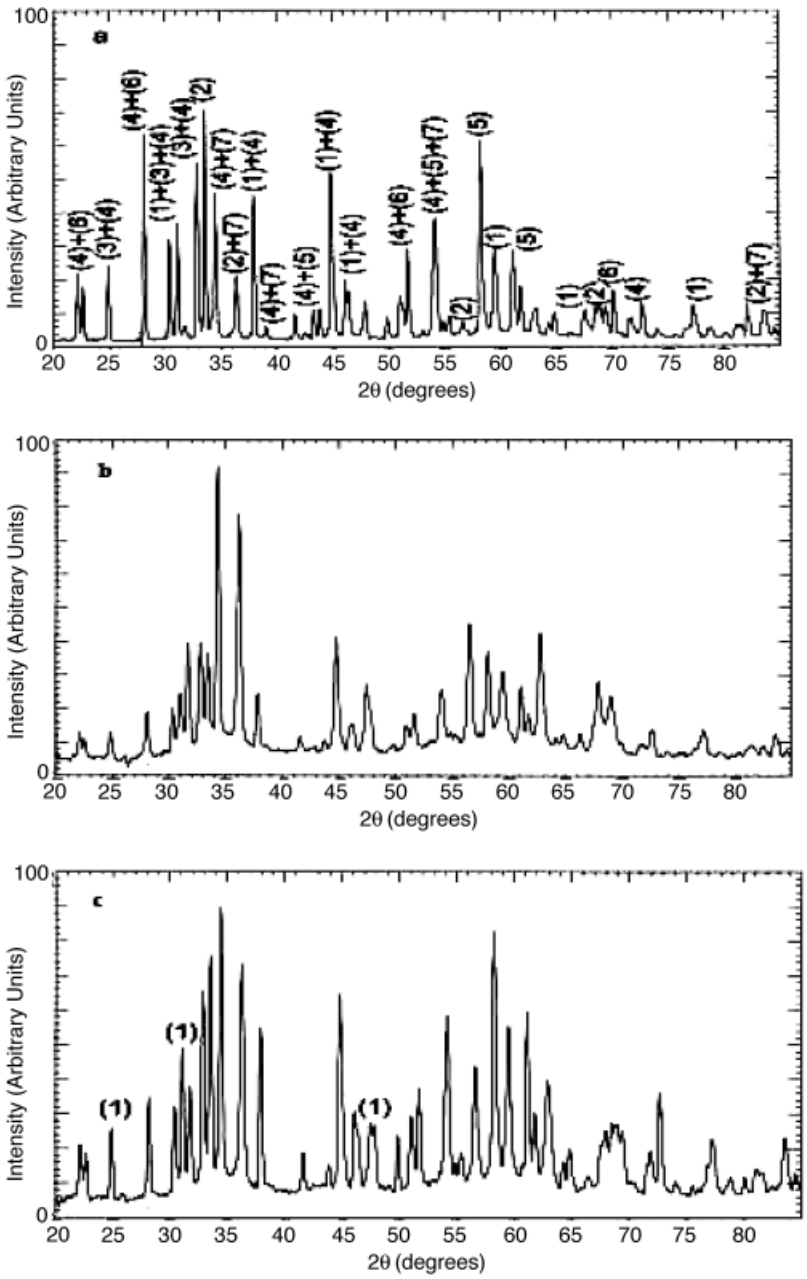

Fig. 7 Selected X-ray diffraction patterns of the coatings formed in galvanizing baths containing a) 0.5 wt% Al, b) 0.5 wt% Sn, and c) 0.5 wt% Cu. The numbers in diffractograph (a) refer to the following compounds: (1) Al_2O_3, (2) ZnO, (3) hydrated Zn compounds, (4) hydrated Zn chlorides and chlorates, (5) Fe oxides, (6) hydrated Fe chlorides, and (7) Zn.

Optical cross-sections (Fig. 4) and SEM micrographs (Fig. 5) verify the heavy damage of the coatings. In some cases (Figs. 4a and c) cavities have been formed, while pits are also present (Figs. 5a and b).

Very useful information was collected from the linear microanalysis of the corroded specimens. In this case the beam of the SEM scanned a line from the zinc–iron interface to the boundary of the coating. The data collected through this method are presented in the form of graphs of an arbitrary unit, which refers

to the quantity of each element in the coating versus the distance from its outer boundary (Fig. 6). These graphs average 10 measurements along the circumference of the coatings.

From the examination of the diagrams of the linear microanalysis (Fig. 6) it was deduced that Na^+ ions are highly diffused in the galvanized coating. The diffusion stops as soon as Na^+ reaches the steel surface. The high diffusivity of this ion is reasonably expected because of its small radius (r^+_{Na} = 0.95 Å [17]). Na^+ does not react with zinc or iron but it enhances corrosion because it increases the conductivity of the water, which is absorbed in the coating.

On the other hand O^{2+} and Cl^- ions appear to distribute uniformly in the coating and they are responsible for the corrosion of both zinc and iron, because of their high reactivity and their high affinity with the two metals. Especially Cl^- is very aggressive because of the high solubility of its compounds [13–16], which enhances internal oxidation phenomena [18].

XRD patterns (Fig. 7) revealed the presence of Zn compounds (such as ZnO, Zn hydroxides, hydrated chlorides, hydrated chlorates, etc.), iron oxides, and hydrated iron chlorides and traces of NaCl. XRD patterns appeared to have small differences depending on the different composition of the zinc bath. For example, in the coating produced from a Zn–Cu bath, hydrated copper chlorides were detected, while in the coatings produced from a Zn–Al bath the presence of Al_2O_3 is clear.

4 Conclusions

– The coatings produced in a Zn–1.0% Al bath are characterized by the existence of an $Fe_2Al_5Zn_x$ layer, which separates the η phase from the steel. This phenomenon is not encountered in the coatings produced in a Zn–0.5% Al bath, where the coating is composed only of ζ and η phases. In both cases inclusions of the chemical formula $FeAl_3$ are trapped in the η phase.

– Concerning the other metals (Pb, Sn, Cu, and Ni), in every case three phases were detected: η, ζ and δ.

– Cu atoms seem to replace Zn atoms in the coating and as a result the Cu quantity in the coating is relatively high.

– Ni atoms act as nucleation sites for the ζ phase. Therefore, Ni favors the formation of a thinner coating with a smooth interface between the ζ and η phases.

– Pb changes the crystallographic orientation of the η phase and also results in the formation of a thinner coating. Hence, the presence of Pb and Ni in the zinc bath diminishes the consumption of zinc, which leads to an important financial benefit.

– Both the appearance and the macroscopic image of all the examined specimens after corrosion are the same. The effect of the corrosive medium is very intense. In some cases even the ferrous substrate is affected.

– The microanalysis of the specimens shows that Na^+ ions are highly diffused into the coatings. O^{2+} and Cl^- ions are more or less uniformly distributed in the coating. This phenomenon is independent of the bath composition.

– The corrosion products are mainly Zn compounds (such as hydroxides, hydrated chlorides, hydrated chlorates, etc.) and Fe compounds (such as oxides and hydrated chlorides). Their composition differs slightly with respect to the bath composition.

References

[1] ASM Handbook, Vol. 13 (ASM, New York, 1999), 432–445.
[2] A. R. Marder, Prog. Mater. Sci. **45**, 191 (2000).
[3] M. Udernicek and J. S. Kirkaldy, Z. Met.kd. **64**, 649 (1987).
[4] N. Katiforis and G. Papadimitriou, Surf. Coat. Technol. **78**, 185 (1996).
[5] G. Reumont et al., J. Mater. Sci. **33**, 4759 (2000).
[6] G. P. Lewis and J. Pedersen, in: Proc. 3rd Asian Pacific Galvanizing Conf., Australia, Cominco Ltd, 1–8 (1996).
[7] J. Strutzenberger and J. Faderl, Metall. Mater. Trans. A **29**, 631 (1998).

[8] F. A. Fasoyino and F. Weinberg, Metall. Trans. B **21**, 549 (1990).
[9] G. Vourlias, N. Pistofidis, G. Stergioudis, and D. Tsipas, in: Proc. Materials Week 2002, Int. Congr. on Advanced Materials, Their Processes and Applications, Symp: Surface Technology, Munich, Germany (2002), No. 467.
[10] Instruction Manual for the Salt Spray Chamber Type SC and Type SC/KWT – Alternative Climate Test Chamber Type SC-450 (Umwelttechnik).
[11] C. E. Jordan and A. R. Marder, J. Mater. Sci. **32**, 5593 (1997).
[12] C. E. Jordan and A. R. Marder, J. Mater. Sci. **32**, 5603 (1997).
[13] S. Oesch and M. Faller, Corros. Sci. **39**, 1505 (1997).
[14] V. Ligier, Corros. Sci. **41**, 1139 (1999).
[15] K. A. van Oetern, Galvanotechnik **72**, 35 (1981).
[16] J. S. Rodriguez, F. J. S. Hernandez, and J. E. G. Gonzalez, Corros. Sci. **45**, 799 (2003).
[17] K. Kabasiadis, General, Theoretical and Electronic Chemistry (Sakoulas, Thessaloniki, 1961), p. 431 (in Greek).
[18] G. Vourlias, N. Pistofidis, G. Stergioudis, E. K. Polychroniadis, and D. Tsipas, J. Opt. Adv. Mater. **6**, 315 (2004).